

## Fermi-Liquid versus Non-Fermi-Liquid Behavior in Triple Quantum Dots

Rok Žitko<sup>1</sup> and Janez Bonča<sup>2,1</sup>

<sup>1</sup>*J. Stefan Institute, Ljubljana, Slovenia*

<sup>2</sup>*Faculty of Mathematics and Physics, University of Ljubljana, Ljubljana, Slovenia*

(Received 12 June 2006; published 23 January 2007)

We study the effect of electron hopping in triple quantum dots modeled by the three-impurity Anderson model. We determine the range of hopping parameters where the system exhibits the two-channel Kondo effect and has non-Fermi-liquid properties in a wide temperature interval. As this interval is entered from above, the conductance through the side dots increases to a half of the conductance quantum, while the conductance through the system remains small. At lower temperatures the conductance through the system increases to the unitary limit as the system crosses over to the Fermi-liquid ground state. Measuring the differential conductance in a three-terminal configuration provides an experimental probe into the NFL behavior.

DOI: [10.1103/PhysRevLett.98.047203](https://doi.org/10.1103/PhysRevLett.98.047203)

PACS numbers: 75.30.Hx, 71.10.Hf, 72.10.Fk, 72.15.Qm

Quantum impurity models describe interaction between a pointlike impurity with internal degrees of freedom and a continuum. The Kondo model of a magnetic impurity accounts for the screening of the impurity spin with decreasing temperature (the Kondo effect). Generalized Kondo models, such as the two-channel Kondo (2CK) model and the two-impurity Kondo (2IK) model, display NFL physics and quantum criticality, which are the central paradigms used to interpret the unusual behavior found in some systems at low temperatures. The 2CK model may explain unusual logarithmic temperature dependence of the magnetic susceptibility and linear vanishing of the quasiparticle decay rate in some Ce and U compounds at low temperatures [1]. The 2IK model was applied to study the competition between magnetic ordering and Kondo screening, which determines the ground state of the heavy-fermion compounds [2].

Quantum dots provide tunable mesoscopic realizations of quantum impurity models [3,4], where the relevant model is usually the ordinary single-channel Kondo or Anderson model [5]. The magnetic moment is either fully screened for a spin-1/2 impurity with Fermi-liquid (FL) ground state or underscreened for a  $S > 1/2$  impurity with a singular FL ground state [6]. Recently, several experimental realizations of the 2CK model using quantum dots have been proposed [7]. In the system of three quantum dots, a small dot embedded between two larger dots, the channel asymmetry can be tuned to small values and NFL behavior was predicted in a limited temperature range [8].

We consider two related systems of three Anderson impurities coupled in series between two conduction channels. We analyze new behavior that results from the presence of two equivalent screening channels combined with either two-stage Kondo screening [3] or magnetic ordering [4], which both lead to a single uncompensated spin at intermediate temperatures. If the impurities are coupled only by exchange interaction, the system has a NFL ground state of the 2CK type with a residual  $\ln 2/2$  entropy [1,9]. In the experimentally relevant case where the exchange inter-

action is generated by the superexchange mechanism due to electron hopping, the channel symmetry is broken and the system is described by the asymmetric 2CK model. We analyze the parameter ranges where NFL behavior is exhibited and identify the regime where the experimental observation is most likely.

*Models.*—We study the three-impurity models described by the Hamiltonian  $H = H_b + H_{\text{imp}} + H_c$ , where  $H_b = \sum_{\nu,k,\sigma} \epsilon_k c_{\nu k \sigma}^\dagger c_{\nu k \sigma}$  describes the left and right conduction lead ( $\nu = L, R$ ) and  $H_c = \sum_{k\sigma} V_k (c_{Lk\sigma}^\dagger d_{1\sigma} + c_{Rk\sigma}^\dagger d_{3\sigma} + \text{H.c.})$  describes the coupling of the bands to the left and right impurity (numbered 1 and 3, while 2 is the impurity in the middle).  $H_{\text{imp}}$  is either the Hubbard Hamiltonian (model I)

$$H_{\text{imp}}^{\text{I}} = \sum_{i=1}^3 \frac{U}{2} (n_i - 1)^2 + \sum_{i=1}^2 \sum_{\sigma} t (d_{i\sigma}^\dagger d_{i+1,\sigma} + \text{H.c.}), \quad (1)$$

where  $U$  is the on-site Coulomb electron-electron repulsion,  $n_i = \sum_{\sigma} d_{i\sigma}^\dagger d_{i\sigma}$  is the electron number on site  $i$  and  $t$  is the interimpurity hopping, or the exchange-only variant of the former (model II)

$$H_{\text{imp}}^{\text{II}} = \sum_{i=1}^3 \frac{U}{2} (n_i - 1)^2 + JS_1 \cdot S_2 + JS_2 \cdot S_3, \quad (2)$$

where  $S_i = \frac{1}{2} \sum_{\alpha\beta} d_{i\alpha}^\dagger \boldsymbol{\sigma}_{\alpha\beta} d_{i\beta}$  is the spin operator on site  $i$  [ $\boldsymbol{\sigma}$  is the vector of Pauli matrices], and  $J$  is the exchange constant. We set  $J$  to the superexchange value of  $J = 4t^2/U$  to relate the two models for  $t \ll U$ . Both models are particle-hole ( $p$ - $h$ ) symmetric. Replacing spin exchange interaction with hopping enables charge transfer between the channels and induces channel asymmetry [8,10] which drives the system to a Fermi-liquid ground state [1].

In model I three different regimes are expected as  $t$  is decreased [11]: molecular-orbital (MO) Kondo regime, antiferromagnetic spin-chain (AFM) Kondo regime and two-stage Kondo (TSK) regime. In MO regime, two elec-

trons occupy bonding molecular orbital, while the third electron in nonbonding orbital develops local moment which is Kondo screened. In the AFM regime, three on-site local moments bind at  $T \sim J = 4t^2/U$  into a rigid antiferromagnetic spin chain with total spin 1/2; this is followed by the screening of the collective spin. In the TSK regime, the moments are quenched successively: on the left and right dot at the upper Kondo temperature  $T_K^{(1)}$ , while on middle dot at an exponentially reduced lower Kondo temperature  $T_K^{(2)}$  [11,12]. All three regimes become qualitatively similar at sufficiently low temperature: the remaining degree of freedom is one spin-1/2 coupled to two Fermi liquids. The most general effective Hamiltonian describing model I that is allowed by the symmetries is the 2CK model with broken channel symmetry. Between TSK and AFM regimes, we identify a wide crossover region where NFL behavior is experimentally most accessible.

Model II has AFM and TSK regimes separated by the crossover regime. There is clearly no MO regime; instead, the AFM regime extends to the region of high  $J$ , where the two models describe very different physical systems. Since the left and right conduction channels are not communicating (in the sense that there are no  $L \leftrightarrow R$  cotunneling processes), the channel symmetry is maintained and a stable 2CK NFL ground state is expected for all  $J$ . In both models (I and II) NFL behavior sets in at the highest temperature in the crossover regime.

**Results.**—We performed calculations using the numerical renormalization group (NRG) method ( $\Lambda = 4$ ) [13]. We assumed a constant density of states  $\rho_0 = 1/(2D)$ , where  $2D$  is the bandwidth, and a constant hybridization strength  $\Gamma = \pi\rho_0|V_{k_F}|^2$ . In Fig. 1 we show the ground state expectation values of charge fluctuations  $(\delta n_i)^2 = n_i^2 - \langle n_i \rangle^2$  and spin-spin correlations between neighboring

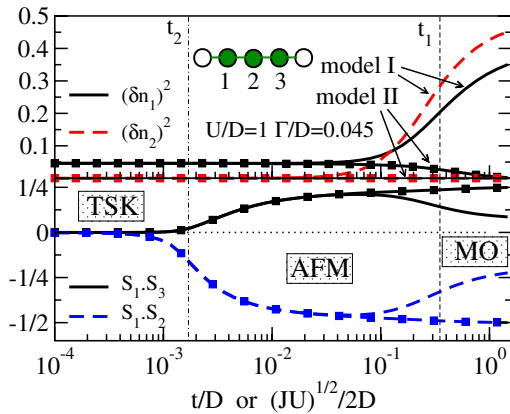


FIG. 1 (color online). Charge fluctuations and spin-spin correlations of model I (lines without symbols) and model II (lines with symbols) as a function of the interdot coupling  $t$  (for model I) or corresponding  $J = 4t^2/U$  (for model II). The MO regime is characterized by large on-site charge fluctuations, the AFM regime by negative spin correlations of neighboring spins 1–2 and positive correlation of spins 1–3, and the TSK regime by vanishing spin correlations.

$\mathbf{S}_1 \cdot \mathbf{S}_2$  and between side impurities  $\mathbf{S}_1 \cdot \mathbf{S}_3$ . For model I, the smooth crossover from MO to AFM regime, predicted to occur on the scale of  $t_1 \sim U/2\sqrt{2} \approx 0.35D$  [11], is reflected in the decrease of charge fluctuations and the increase of spin-spin correlations. The crossover from AFM to TSK regime occurs when  $J \sim T_K^{(1)}$  or  $t_2 \sim 1.710^{-3}D$ : as  $t$  decreases past  $t_2$  the spin-spin correlations tend toward zero as the spins decouple. For model II, while in the AFM regime near  $t \sim t_1$  the differences become notable. Large values of  $J \gg \Gamma$  suppress charge fluctuations on side-dots,  $(\delta n_1)^2 \rightarrow 0$ , while local moments on impurities tend to form a well developed AFM spin-chain (for comparison, in isolated three-site spin chain  $\langle \mathbf{S}_1 \cdot \mathbf{S}_2 \rangle = -1/2$  and  $\langle \mathbf{S}_1 \cdot \mathbf{S}_3 \rangle = 1/4$ ).

In Fig. 2 we plot the impurity contribution to susceptibility and entropy. The ground state of model I is non-degenerate,  $s_{\text{imp}} = 0$ , and the impurities are fully screened for all  $t$ . In the MO regime the system undergoes single-channel Kondo screening with  $T_K$  that increases with  $t$  and becomes constant for  $t \gg U$ , see Fig. 3. In the AFM regime, the binding of spins is most clearly discernible in the curves calculated at  $t/D = 0.05$  which show a kink in  $s_{\text{imp}}$  at  $3 \ln 2$  (local moment formation), followed by an exponential decrease to  $s_{\text{imp}} = \ln 2$  at  $T \sim 4t^2/U$ . The Kondo screening in the AFM regime is of the single-channel type for  $t/D \gtrsim 0.02$ . Between  $t/D = 0.02$  and  $t_2$

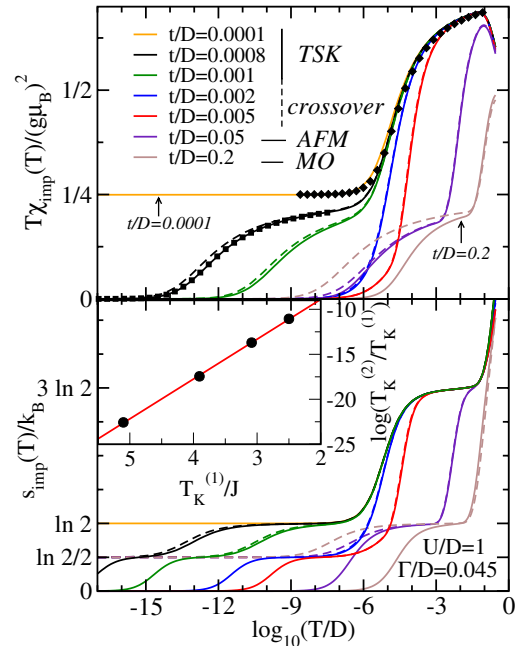


FIG. 2 (color online). Impurity susceptibility and entropy for model I (full lines) and model II (dashed line) with  $J = 4t^2/U$ . Lozenges  $\blacklozenge$  are a fit to Bethe-Ansatz results for one-channel Kondo model (multiplied by two and shifted by 1/4) and squares  $\blacksquare$  are a fit to NRG results for 2CK model. Inset:  $T_K^{(2)} = aT_K^{(1)} \exp(-bT_K^{(1)}/J)$  scaling of the second Kondo temperature of model I.  $a = 0.97$ ,  $b = 4.4$ ,  $T_K^{(1)}/D \approx 1.010^{-5}$ .

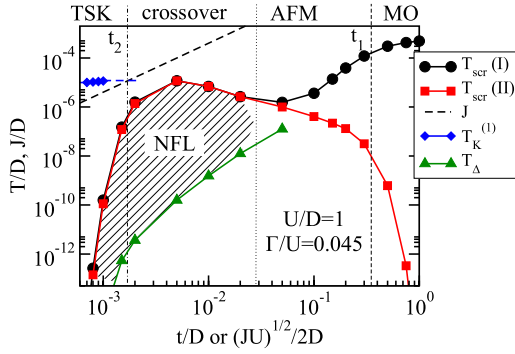


FIG. 3 (color online). Crossover scales of models I and II as functions of the interdot coupling. The magnetic screening temperature  $T_{\text{scr}}$  is defined by  $T_{\text{scr}}\chi(T_{\text{scr}})/(g\mu_B)^2 = 0.07$ ; it is equal to the Kondo temperature when screening is due to the single-channel Kondo effect.  $T_{\Delta}$  is here defined as  $s_{\text{imp}}(T_{\Delta})/k_B = \ln 2/4$ .

there is a *crossover regime* with NFL-like properties. Here magnetic ordering competes with the single-channel Kondo screening of left and right impurity. The magnetic moment is rapidly quenched at  $T \sim T_{\text{scr}} \sim J$ , yet the entropy does not go to zero but exhibits a  $\ln 2/2$  NFL plateau. At still lower temperature  $T_{\Delta}$ , NFL fixed point is destabilized by the channel asymmetry and the system crosses over to the FL ground state characteristic of the conventional Kondo model. Note that in this regime  $T_{\text{scr}}$  is high while  $T_{\Delta}$  is low (Fig. 3), making this range suitable for experimental study of NFL physics.

In the TSK regime, the left and right impurity are screened by the single-channel Kondo effect at temperature  $T_K^{(1)}$  that is nearly the same for all  $t \leq t_2$  (Fig. 3). The central impurity is screened by the 2CK effect at  $T_K^{(2)}$ , below which the system is near the NFL fixed point with  $\ln 2/2$  entropy. In the inset to Fig. 2 we show that  $T_K^{(2)}$  scales as  $T_K^{(2)} \propto T_K^{(1)} \exp(-bT_K^{(1)}/J)$ , as expected for the TSK effect [12].

Model II has a stable NFL ground state. For low  $J$ , it has a TSK regime where the Kondo temperature  $T_K^{(2)}$ , determined by  $J$ , is lower than that of the corresponding model I (Fig. 3). In the *crossover regime* physical properties of model II for  $T > T_{\Delta}$  match closely those of model I. In the AFM regime, the Kondo temperature is a nonmonotonic function of  $J$ . The energy required to break the doublet spin-chain state increases with  $J$  and the effective Kondo exchange constant  $J_K \propto \Gamma/J$  decreases.  $T_K$  therefore decreases exponentially with increasing  $J$ .

*Fixed points.*—By comparing NRG eigenvalue flows, we have verified that for any  $t \neq 0$  the model I flows to the same strong coupling FL fixed point. The spectrum is a combination of two FL spectra: one for odd-length and one for even-length free electron Wilson chain [13]. The odd channel gathers a  $\pi/2$  phase shift, while the even channel has zero phase shift. Since the conductance is given by  $G = G_0 \sin^2(\delta_o - \delta_e)$  with  $G_0 = 2e^2/h$ , the system is fully conducting at  $T = 0$  for any nonzero  $t$ . Weak pertur-

bations of the form  $H' = Vn_i$  are marginal, therefore the triple quantum dot system has an extended region of high conductance as a function of the gate voltage [11]. The unstable intermediate temperature fixed-point spectrum of model I is in agreement with the conformal field theory predictions for the 2CK model [9] (Fig. 4). The same fixed point is obtained for all  $J$  in model II.

*Robustness of the NFL regime.*—In model I, the channel symmetry is broken intrinsically by the interimpurity hopping, which contributes a left-right cotunneling term of the form  $J_{LR}\mathbf{S} \cdot (\mathbf{s}_{LR} + \mathbf{s}_{RL})$  to the effective Hamiltonian ( $\mathbf{s}_{LR}$  is the left-right spin operator  $\mathbf{s}_{LR} = \frac{1}{2} \sum_{kk'\alpha\beta} c_{Lk\alpha}^\dagger \boldsymbol{\sigma}_{\alpha\beta} c_{Rk'\beta}$ ) [8]. The impurities then couple to a symmetric and antisymmetric combination of channels with exchange constants  $J_{S,A} = J_{\text{avg}} \pm J_{LR}$ . The asymmetry parameter  $A = \Delta/\mathcal{J}^2$  with  $\Delta = \rho_0(J_S - J_A) = 2\rho_0 J_{LR}$  and  $\mathcal{J} = \rho_0(J_S + J_A)/2 = \rho_0 J_{\text{avg}}$  determines the crossover scale  $T_{\Delta}/T_K \approx A^2$  [5]. Estimating  $J_S$  and  $J_A$  for  $t/D = 0.005$  using the Schrieffer-Wolff transformation we obtain  $A^2 \sim 10^{-6}$ , to be compared with  $T_{\Delta}/T_{\text{scr}} \sim 10^{-5}$  determined by the NRG calculation. The discrepancy appears due to competing magnetic ordering and Kondo screening (and emerging two-stage Kondo physics); simple scaling approach fails in this case.

We have performed a range of calculations for various perturbations for  $t/D = 0.005$ . The  $\ln 2/2$  NFL plateau persists even for large deviations from the  $p$ - $h$  symmetry ( $H' = V \sum_i n_i$  up to  $V/U \approx 0.2$ ), for broken left-right symmetry or parity ( $H' = V(n_1 - n_3)$  up to  $V/U \approx 0.2$ ), and for unequal on-site repulsion parameters  $U_i$ . The only “dangerous” perturbations are those that increase the channel asymmetry; these can be compensated in experiments by tuning electrode voltages.

*Transport properties.*—The qualitative temperature dependence of the zero-bias conductance through the system can be inferred in a very rough approximation from the frequency dependence of the spectral functions. The conductance through the system is given by

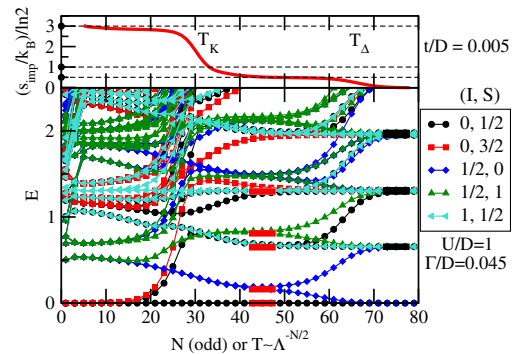


FIG. 4 (color online). NRG eigenvalue flow of model I ( $\Lambda = 2$ ,  $z = 1$ ) in the crossover regime (below) and the corresponding impurity entropy (above). The states are classified according to the total isospin and total spin quantum numbers,  $(I, S)$ . Black full strips correspond to FL spectrum. Gray (red online) hatched strips are at energies (after rescaling by  $1.296$ )  $\frac{1}{8}$ ,  $\frac{1}{2}$ ,  $\frac{5}{8}$ ,  $1$  [9].

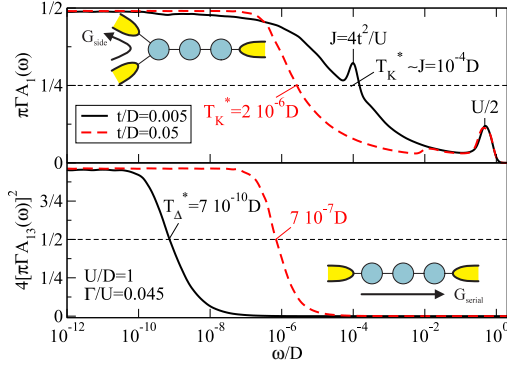


FIG. 5 (color online). Dynamic properties of model I in the AFM (dashed lines) and in the crossover regime (full lines). Upper panel: on-site spectral function  $A_1(\omega)$  of the left dot. Lower panel: out-of-diagonal spectral function  $A_{13}(\omega)$  squared. Temperature  $T_\Delta^*$  is of order  $T_\Delta$ ,  $T_K^*$  is of order  $T_{scr}$ .

$G_{serial}/G_0 \approx 4(\pi\Gamma A_{13})^2$  [14] and the conductance through a side dot in three-terminal configuration by  $G_{side}/G_0 \approx \pi\Gamma A_1$  [15]. The appropriately normalized spectral densities are shown in Fig. 5 for the cases of crossover regime with a NFL region and AFM regime with no discernible NFL behavior. In the NFL region ( $t/D = 0.005$  and  $T_\Delta \leq T \leq T_{scr}$ ), the conductance  $G_{side} \sim 1/2G_0$ , while  $G_{serial} \sim 0$ . The increase of the conductance through the system at  $T \leq T_\Delta$  is concomitant with the crossover from NFL to FL fixed point, since charge transfer (or, equivalently, channel asymmetry) destabilizes the NFL fixed point as in the two-impurity case [10]. In the AFM regime with no NFL region, both conductances increase below the same temperature scale, i.e.,  $T \leq T_{scr}$ .

In  $A_1(\omega)$ , the Hubbard peak at  $U/2$  corresponds to adding an electron to the site, while the “magnetic-excitation” peak at  $J$  appears when, after adding an electron, the electron with the opposite spin hops from the impurity into the band. This breaks the AFM spin chain, increasing the energy by  $J$ . This magnetic peak evolves into a “molecular-orbital” peak at the energy of the nonbonding orbital (for  $t$  in MO regime) or into the Kondo peak of the side dot (for  $t$  in TSK regime).

**Conclusion.**—In a wide interval around the  $p$ - $h$  symmetric point, the triple quantum dot system has a FL ground state with high conductance at  $T = 0$ . The different regimes exhibit different approaches to this fixed point. The most likely candidate for observing 2CK behavior is the crossover regime with competing magnetic ordering and Kondo screening,  $J \sim T_K$ . In this regime the NFL behavior occurs in a wide temperature range and it is fairly robust against various perturbation that do not additionally increase the channel asymmetry. The signature of the NFL behavior can be detected by measuring  $G_{side}$  and  $G_{serial}$  in a three-terminal configuration. Properly choosing parameters of the triple quantum dot system to set it into the crossover regime represents a road map for observation of NFL behavior.

We remark that all systems of quantum dots described as Kondo or Anderson impurities that are coupled to two noninteracting leads belong to the same class of quantum impurity problems with four (spin and channel) flavors of bulk fermions [2, 16]. The boundary conformal field theory approach allows for systematic determination of all possible nontrivial (NFL) fixed points. It would be interesting to investigate the *inverse problem* of finding the microscopic Hamiltonians which renormalize to these points. Since renormalization-group transformations are not invertible, this appears as a formidable task that would involve considerable guesswork. Nevertheless, its resolution would provide important insight into a variety of possible experimental realizations of mesoscopic NFL systems with *purely local* interactions.

The authors acknowledge useful discussions with A. Ramšak and the financial support of the SRA under Grant No. P1-0044.

- 
- [1] D. L. Cox and A. Zawadowski, *Adv. Phys.* **47**, 599 (1998).
  - [2] B. A. Jones, C. M. Varma, and J. W. Wilkins, *Phys. Rev. Lett.* **61**, 125 (1988); I. Affleck, A. W. W. Ludwig, and B. A. Jones, *Phys. Rev. B* **52**, 9528 (1995).
  - [3] W. G. van der Wiel *et al.*, *Phys. Rev. Lett.* **88**, 126803 (2002).
  - [4] N. J. Craig *et al.*, *Science* **304**, 565 (2004).
  - [5] M. Pustilnik and L. Glazman, *J. Phys. Condens. Matter* **16**, R513 (2004).
  - [6] W. Koller, A. C. Hewson, and D. Meyer, *Phys. Rev. B* **72**, 045117 (2005); P. Mehta, N. Andrei, P. Coleman, L. Borda, and G. Zarand, *Phys. Rev. B* **72**, 014430 (2005).
  - [7] Y. Oreg and D. Goldhaber-Gordon, *Phys. Rev. Lett.* **90**, 136602 (2003); F. B. Anders, E. Lebanon, and A. Schiller, *Phys. Rev. B* **70**, 201306(R) (2004); M. Pustilnik, L. Borda, L. I. Glazman, and J. von Delft, *Phys. Rev. B* **69**, 115316 (2004); C. J. Bolech and N. Shah, *Phys. Rev. Lett.* **95**, 036801 (2005).
  - [8] T. Kuzmenko, K. Kikoin, and Y. Avishai, *Europhys. Lett.* **64**, 218 (2003).
  - [9] I. Affleck, A. W. W. Ludwig, H.-B. Pang, and D. L. Cox, *Phys. Rev. B* **45**, 7918 (1992).
  - [10] G. Zarand, C.-H. Chung, P. Simon, and M. Vojta, *Phys. Rev. Lett.* **97**, 166802 (2006).
  - [11] R. Žitko, J. Bonča, A. Ramšak, and T. Rejec, *Phys. Rev. B* **73**, 153307 (2006).
  - [12] M. Vojta, R. Bulla, and W. Hofstetter, *Phys. Rev. B* **65**, 140405(R) (2002); R. Žitko and J. Bonča, *Phys. Rev. B* **73**, 035332 (2006); P. S. Cornaglia and D. R. Grempel, *Phys. Rev. B* **71**, 075305 (2005).
  - [13] K. G. Wilson, *Rev. Mod. Phys.* **47**, 773 (1975).
  - [14] C. Caroli, R. Combescot, P. Nozières, and D. Saint-James, *J. Phys. C* **4**, 916 (1971).
  - [15] Y. Meir, N. S. Wingreen, and P. A. Lee, *Phys. Rev. Lett.* **70**, 2601 (1993).
  - [16] J. M. Maldacena and A. W. W. Ludwig, *Nucl. Phys.* **B506**, 565 (1997).